

Implications of recent solar neutrino observations: an analysis of charged current data

C. V. K. Baba*, D. Indumathi and M. V. N. Murthy
The Institute of Mathematical Sciences, Chennai 600 113, India.
 (Jan 1, 2002)

Abstract

We have analysed the recent results from the observation of charged current $\nu_e d \rightarrow e^- pp$ events from solar neutrinos by the Sudbury Neutrino Observatory SNO assuming neutrino oscillations with three active flavours. The data seem to prefer a low mass-squared difference and large mixing angle solution (the so-called LOW solution) in (12) parameter space. However, when combined with the Gallium charged current interaction data from Gallex and GNO, distinct (1σ) allowed regions corresponding to the large mixing angle (LMA) and small mixing angle (SMA) appear while the LOW solution is disfavoured upto 3σ standard deviation. The physical electron neutrino survival probability corresponding to these best fit solutions are then determined and analysed for their energy dependence.

Typeset using REVTeX

*Permanant address: Nuclear Science Centre, New Delhi 110 067

I. INTRODUCTION

The recent announcement of results on the observation of charged current (CC) neutrino events from the sun by the Sudbury Neutrino Observatory (SNO) [1] has lead to a flurry of activity in understanding the implications of the data on neutrino oscillations. Several authors have concentrated on the global analysis [2] of the solar neutrino data from all existing observations and the refinement in the allowed oscillation parameter space. Typically, such analyses have refined the already existing allowed regions in parameter space—the so-called small mixing angle (SMA), large mixing angle (LMA), Low Mass (LOW) and the ‘just so’ solutions. However, not as much attention has been paid to how individual experimental results perform with respect to the best possible global fits.

This paper is not devoted to providing yet another global best fit. We concentrate rather on the *physical* quantity of interest, viz., the neutrino survival probability. Since we restrict ourselves to the CC data, we focus on the electron neutrino survival probability, $P_{ee}(E_\nu)$. The question that we seek to address is, what are the constraints from data on the energy dependence of P_{ee} . In order to answer this question, we use the energy integrated CC data from the combined Gallium experiments of GALLEX and GNO¹ [4] (henceforth referred to as the Ga experiments) as well as the recent CC observations from SNO [1]. We also briefly discuss the constraints arising from the Homestake Chlorine experiment [5] (henceforth called Cl). We do not include the results from Super-Kamiokande in our analysis since the observed elastic scattering process has both CC and neutral current (NC) components. We use the standard solar model of BP2001 in our theoretical analysis; the flux data are available in tables at the web-site [6].

Of these experiments, the Ga experiments observe neutrinos over the widest range of energies. However, the Ga data contain no energy information. Theoretically, the bulk of the events may be attributed to electron neutrinos with energy less than 1 MeV with less than 10% coming from neutrinos with energy more than 5 MeV. On the other hand SNO observes only the ⁸B neutrinos above a threshold of about 8 MeV. It is also sensitive (indirectly) to the neutrino energy. In short, these experiments are sensitive to different source reactions in the sun. We can therefore get good information by analysing the combined data as well as the individual data sets. The Cl experiment is sensitive to the (second) ⁷Be line apart from the B neutrino flux. Like Ga, it does not contain any energy information. However, it turns out that Cl and SNO yield similar likelihood curves in the allowed parameter space.

We first analyse the experiments individually and then the combined Ga and SNO data. We have used simple expressions for the likelihood contours where the χ^2 is defined using diagonal errors only; all correlated errors are ignored. This approximation is obviously valid for SNO since there is exactly one contributing source flux; it remains true to good accuracy for Ga since the dominant low energy pp source flux has very small errors. Finally, since there is only 10% overlap between the Ga and SNO source fluxes, the neglect of correlated errors is valid while analysing the combined data as well. This is not true for the combined Ga, Cl and SNO data sets; hence we have not presented the results of such a combined

¹We have used the cited average of these data; the SAGE Gallium experiment [3] is also consistent with these data.

analysis here.

Assuming that neutrino oscillations are the source of the discrepancy between data and theory, we find that the likelihood contours in the allowed parameter space for the Ga experiments differ substantially from the SNO and Cl ones. Consequently, it turns out that the electron neutrino survival probability (the CC analysis depends only on this probability) corresponding to the best fit parameters (χ^2 minimum) has a very different energy dependence for the fits coming from analysing the Ga or SNO data alone and the combined fits. This is true especially for the so-called LMA solution where the SNO prefers a rather flat P_{ee} while Ga shows a distinct energy dependence. This leads to the question whether the low energy pp neutrinos behave very differently from the higher energy ones. If so, it is possible that a measurement of the (second) ${}^7\text{Be}$ line spectrum will be able to settle this issue. For example, an almost vanishing ${}^7\text{Be}$ flux ($< 10\text{--}20\%$ of the expected flux) will point unambiguously to the SMA as the preferred solution to the neutrino oscillation problem. A similar analysis for the best-fit global solutions may be found in Ref. [7].

In Section 2, we present the relevant formulae for the event rate as well as for the survival probability of (e-flavour) neutrinos in the 3-flavour oscillation scheme. In Section 3 we present the results of the numerical calculation using the standard solar model of BP2001 [6] for the solar neutrino fluxes. Section 4 contains the summary and discussion.

II. RELEVANT FORMULAE

We briefly list the relevant formulae in a 3-flavour oscillation scenario to explain the discrepancy between data and theory. The mixing is expressed as,

$$\begin{pmatrix} \nu_e & \nu_\mu & \nu_\tau \end{pmatrix}^T = V \times \begin{pmatrix} \nu_1 & \nu_2 & \nu_3 \end{pmatrix}^T ,$$

where the mass eigenstates ν_i have masses m_i and the mixing matrix is parametrised in terms of three angles² as a set of 3 independent 2×2 rotations:

$$V = V_{23}(\psi) \times V_{13}(\phi) \times V_{12}(\omega) .$$

The angle ψ does not occur in expressions for solar neutrinos since only ν_e neutrinos are produced in the sun.

Since we are interested only in the CC events, the only relevant probability is the electron neutrino survival probability, P_{ee} . This can be expressed in terms of the (12) and (13) mixing angles, ω and ϕ , as well as the (12) mass squared difference, $m_2^2 - m_1^2 = \delta_{12}$. We have

$$P_{ee} = \sin^2 \phi \sin^2 \phi_m + \cos^2 \phi \cos^2 \phi_m \left[\frac{1}{2} + \left(\frac{1}{2} - P_{LZ} \right) \cos 2\omega \cos 2\omega_m \right] . \quad (1)$$

Here the subscript m includes the usual (solar) matter effects. We do not include earth matter effects here; this affects only the ‘LOW’ solution and that too, at a small level. Here P_{LZ} is the non-adiabatic jump probability [8] and is relevant near resonance. While

²We ignore the CP violating phase here.

$\cos 2\phi_m \sim \cos 2\phi$, $\cos 2\omega_m$ depends on the vacuum mixing angles as well as δ_{12} and the matter term $A(E_\nu)$. Hence it is energy dependent. Note that we have used the phase averaged expression for P_{ee} ; this is allowed as long as we restrict ourselves to $\delta_{12} > 10^{-8}$ eV². Hence we do not consider the ‘just-so’ solutions in this paper. Finally, $A(E_\nu)$ is also density dependent [8]. The solar density varies with distance; however, we have used average values of density corresponding to the peak production of different source fluxes since we have averaged over the production region. The results are not sensitive to this approximation [8].

The survival probability appears in the expression for the ratio:

$$R^{\text{th}} = \frac{\int dE_\nu P_{ee}(E_\nu) \phi(E_\nu) \sigma(E_\nu)}{\int dE_\nu \phi(E_\nu) \sigma(E_\nu)}, \quad (2)$$

where the factor $(P_{ee} \phi)$ in the numerator represents the depleted flux due to mixing and depends on the mixing parameters as shown; σ is the cross-section for the relevant process in the detector; σ may also be differential with respect to one or more variables as in the case of the SNO data where we use $d\sigma/dE_e$, with E_e the scattered electron energy. There is a further smearing out of this data due to the resolution function since the measured electron energy E_e is a gaussian distributed around the true electron energy E'_e [1]. The Ga cross-section is taken from tables available in Ref [9]. The deuterium cross-section is taken from the tables available in Ref. [10].

The theoretical value of R^{th} calculated this way is then compared with the ratio R^{exp} measured by the different experiments³. To avoid double counting, the theoretical errors were factored into R^{th} while the experimental numbers included only the statistical errors.

The significance of SNO and Gallex for mass and mixing parameters is obtained by separately determining the minimum χ^2 , where we use the standard definition

$$\chi^2 = \sum_{\alpha} \frac{(R_{\alpha}^{\text{th}} - R_{\alpha}^{\text{exp}})^2}{\sigma_{\alpha}^2}, \quad (3)$$

where the explicit parameter dependence of the ratio is $R_{\alpha}^{\text{th}} = R_{\alpha}^{\text{th}}(\delta_{ij}, \theta_{ij})$ for a given set of mass squared differences, δ_{ij} , and mixing angles, θ_{ij} . The range of the subscripts is determined by the number of neutrino flavours. For P_{ee} we have the three parameters δ_{12} , ω and ϕ . The subscript α runs over the set of data points, R_{α}^{exp} , of a given experiment(s). The theoretical and experimental errors are added in quadrature in σ_{α}^2 . Likelihood contours are drawn using

$$\mathcal{L} = \exp \left[-\chi^2/2 \right].$$

While \mathcal{L} by itself has no meaning (it is the log likelihood or χ^2 itself that is relevant), $n\sigma$ likelihood contours can be drawn corresponding to $\chi^2 = \chi_{\text{min}}^2 + n^2$. These contours have the

³The SNO ratio is calculated using the same BP2001 model. The experimental event rate in SNUs for the Ga (actually the average from Gallex and GNO) and Cl experiments were used and converted to a ratio using the BP2001 calculated prediction.

usual probability interpretation of allowed regions. We use the parameters corresponding to the best fit (and within 1σ of the best fit) to find the preferred survival probability.

As we have observed, all charged current events are directly proportional to the electron neutrino survival probability. This is not true for the case of the Super-Kamiokande data in the presence of an additional sterile flavour; analysis of this data would require an additional unknown, the oscillation of ν_e into the sterile flavour. This is why an analysis of charged current data provides the most restrictive bounds on the mixing.

III. NUMERICAL ANALYSIS AND RESULTS

A. Choice of data

We have individually analysed the following sets of solar neutrino data: CC data from SNO (referred to as SNO data), from the Gallium detectors GALLEX and GNO (referred to as Ga data), and from the Chlorine detector at Homestake (referred to as Chlorine data). All these experiments measure charged current data (we have not analysed the SNO elastic scattering data here) and hence are particularly tuned to the electron-type neutrinos. The data are expressed as ratios of observed to expected event rates. We use the BP2001 [6] standard solar model for the theoretical calculation.

Energy integrated data from Ga and Cl (with $E_{\nu,\min} = 0.24$ and 0.814 MeV respectively) yield one data point from each experiment while SNO (apart from an energy integrated value for the ratio of observed to expected rate) also gives data in 11 bins for the recoil electron energy starting from E_e of about 7.25 MeV, with bin size about 0.51 MeV (except for the last bin) [1]. The Q value for the reaction $\nu_e d \rightarrow e p p$ is 0.93 MeV, so the parent neutrino energy is at least 8 MeV; it is however useful to note that the cross-section for this reaction peaks typically at $E_e = E_\nu - 1.4$ MeV [10] although the peak value is mildly energy dependent. Hence there is good energy information in the SNO data.

As pointed out earlier, SNO sees only the ^8B neutrinos from the sun, Chlorine also sees most (about 90%) of the Be neutrinos and Ga sees both Be and B and much of the pp neutrinos. In our analysis, we have ignored errors due to correlations between the different fluxes (that would not affect SNO) contributing to the event rate at any given experiment. We have also used only the statistical errors in the data (since, typically, systematic errors are also correlated between data bins). Hence the χ^2 minima that we compute are a lower bound on that which would have been obtained if the correlated errors were taken into account.

Also, as pointed out in the Introduction, it is possible to do a combined analysis of the Ga and SNO data while still ignoring correlated errors. This has also been done.

B. Allowed Parameter Space

We begin by finding the allowed parameter space for the individual data sets. These are shown in Figs. 1 where the allowed 1σ regions of δ_{12} and ω around the global minimum χ^2 are shown for $\phi = 0$. There is not much sensitivity to ϕ in the range allowed by CHOOZ, $\phi \leq 9^\circ$ [11]. The 2σ regions (not shown in the figure) are quite large, especially for the Ga

and Cl data sets since there is exactly one data point (total rate) available. While it may appear that one data point is being fitted with two (or even three) free parameters for Ga and Cl, the resulting restriction in parameter space occurs because of the non-trivial energy dependence of P_{ee} and the fact that different source fluxes contribute differently at different energies. For the SNO data, we have shown the region of parameter space allowed by taking into account either all the 11 electron energy bins or the integrated rate. Obviously, the allowed region is larger if only the average (integrated) rate is taken into account, as shown in the figure. However there is a good overlap between these two fits, indicating the stability of the fits.

There is almost complete overlap between the allowed parameter space from Chlorine and SNO data especially at large angles. The contribution to Cl from the region below the SNO threshold comes roughly equally from the (second) ${}^7\text{Be}$ line spectrum and from a part of the ${}^8\text{B}$ flux. The overlap between the two sets therefore seems to indicate that the nature of suppression in the SNO energy regime is similar to that at lower energies, down to the Cl threshold. The SNO energy-dependent data are more restrictive; the effect of this is to allow a narrower strip of parameters than the Chlorine data.

What is interesting is that the preferred regions for Ga and Chlorine/SNO are totally different as can be seen by comparing the relevant panels of Fig. 1. The so-called LMA solution for Ga has a well-defined $\omega \sim 25^\circ$ but accomodates a large range of δ_{12} , $\delta_{12} > 10^{-5} \text{ eV}^2$. Solutions corresponding to the SMA exist although the SMA region is not distinct from the LMA one; however, the LOW solution (corresponding to low mass squared, large angle) is conspicuously absent in Ga.

Even more surprisingly, while SNO shows allowed regions in the regions corresponding to SMA, LMA and LOW, these regions are connected with no well-defined LMA or SMA minima. The global minimum for the entire region is in fact the so-called LOW solution centred around $\delta_{12} \sim 6.7 \times 10^{-8} \text{ eV}^2$ and $\omega \sim 29^\circ$.

In general, the SMA and LMA allowed regions of SNO and Ga are different. Hence, when the Ga and SNO data are combined distinct regions in LMA and SMA parts of the parameter space appear (see Table 1). Since Ga does not have a LOW solution, the ‘LOW’ solution (that is in fact the global minimum of the fits to the SNO data) is completely disallowed by the combination of Ga and SNO data by about 4σ . The SMA solution is marginally preferred over the LMA. However, in our simple analysis we have neglected correlations as well as earth matter effects. Though small, this precludes us from preferring SMA over LMA; within the errors of the analysis both are equally likely.

The result from the combined fit is shown in Fig. 2. Note that since we have ignored correlations between the fluxes, the allowed regions are just the overlaps of the separately allowed regions. In the figure, the 1σ allowed contours (with respect to the local χ^2 minima) are shown in the δ_{12} - ω plane for fixed $\phi = 0^\circ, 9^\circ$, and 20° . The solid lines correspond to the combined analysis of Ga and SNO energy-binned data, while the dotted lines correspond to the combined Ga and integrated SNO data. As expected, the allowed region shrinks when the energy dependence of the SNO data is taken into account. We have also analysed the Ga data together with data in the higher energy bins of SNO (from the 5th to the 11th bin in the recoil electron energy). This is because the correlated errors are significant (compared to the statistical errors) amongst the first four bins and negligible for the rest. Hence our neglect of correlated errors is strictly valid only for these bins. The result of such an

analysis (for $\phi = 0$) is very similar to the analysis using the entire SNO data set and is shown in Fig. 2 as dashed lines in the second panel. This leads us to believe that our results are not very sensitive to inclusion of correlations.

Also, for the LMA solution, the χ^2 is smallest for $\phi = 0^\circ$, increasing with increasing ϕ ; the opposite behaviour is seen for the SMA solution. In both cases, however, there is a decrease in the allowed region with increasing ϕ . This provides a loose bound on ϕ , $\phi < 20^\circ$, independently of CHOOZ data. This is also seen from the global minimisation with respect to all three free parameters. The LMA best fit yields $\phi \sim 0$ with a 1σ error of about 23° as can be seen from Table 1.

C. The survival probability

The probability shapes corresponding to these preferred solutions are shown in Figs. 3 and 4. The two figures correspond to the so-called large mixing angle (LMA and LOW) solutions and the small mixing angle (SMA) solutions. While all three solutions are allowed only by SNO, Ga has a preferred SMA and LMA solution, whose corresponding P_{ee} is shown in the figures. The P_{ee} corresponding to the χ^2 minimum from the combined Ga-SNO analysis is shown as solid lines in the figures. The two lines per solution correspond to the 1σ limits on the parameter values and indicate the range of P_{ee} allowed.

The energy corresponding to the (second) ${}^7\text{Be}$ line is indicated on both the figures for LMA/LOW and SMA solutions. The LMA and SMA solutions clearly show that roughly 60% and 10% respectively of the total Be flux will survive and be detected at Borexino, for example. Even beyond the 1σ level, a low (less than about 30%) fraction of ${}^7\text{Be}$ will indicate a clear preference for the SMA solution. Hence a measurement of the Be flux will be crucial in distinguishing the LMA and SMA solutions and in narrowing down the allowed parameter space for mixing.

It is seen that the results of the combined analysis are driven mostly by the SNO data. Hence the errors on the P_{ee} are smaller at larger energies where SNO data are available. In particular, while still being well within the range allowed by the Ga SMA solution, the allowed P_{ee} range from the SNO SMA solution at larger energies is very restricted as can be seen from Fig. 4.

The fits favoured by Ga data, on the other hand, tend to either underestimate (Ga-LMA) or allow a very broad band of P_{ee} in the energy range relevant for SNO. The reason for this is obvious: there is no energy information in the Ga data. In spite of this, it is able to rule out the LOW solution for SNO. (On the average, the Ga data corresponds to lower energy of roughly $\langle E_\nu \rangle \sim 0.3$ MeV. The observed Ga ratio which is 0.58 ± 0.07 cannot therefore be accommodated by the LOW solution as can be seen from Fig. 3).

Another way of understanding this is to look at the likelihood contours for the combined Ga-SNO fits over the entire parameter region. We have shown this in Fig. 5 for $\phi = 0$. The likelihood contours corresponding to $n\sigma$ allowed regions, $n = 1, 10$, with respect to the global minimum (see Table 1) are shown in the δ_{12} vs $\tan^2 \omega$ (or ω) plane. The 1σ contours show the two distinct SMA and LMA allowed regions very clearly. It is seen that the minimum corresponding to SMA is very narrow. The LMA region is larger and smoothly goes into the so-called “LOW” at 4σ . Hence the LOW solution is allowed only at 4σ . The results are not very different for $\phi = 9^\circ$.

IV. SUMMARY

We have performed an analysis of the charged current SNO and Gallium solar neutrino data with a view to understanding the physically allowed electron neutrino survival probability assuming an oscillation hypothesis with 3 active neutrino flavours. We have analysed the data separately as well as done a combined fit. The results can be summarised as follows.

- The data are not very sensitive to the (13) mixing angle, ϕ . However even if we do not apply the CHOOZ bound [11], $\phi < 9^\circ$, very large $\phi > 20^\circ$ does not seem compatible with the SNO/Ga data.
- The individual Gallium and SNO (as also the Chlorine data) give rise to very different allowed regions of parameter space. These regions are contiguous with no distinct LMA and SMA regions visible (see Fig. 1).
- In particular the so-called 'LOW' solution (small (12) mass-squared difference, δ_{12} , large (12) mixing angle, ω) is totally incompatible with the Ga data although it is the preferred solution for SNO. A combined analysis of the SNO and Ga data rules out this solution at 4σ .
- Distinct small angle and large angle solutions (SMA and LMA) appear on combining the Ga and SNO data sets. Both solutions are equally preferred.
- Finally, the currently allowed SMA and LMA solutions predict very different survival probability of the (second) ^7Be line spectrum. An exclusive measurement of the ^7Be flux such as from Borexino will be able to distinguish whether the small angle solution or the large angle solution is ultimately the right solution.

Due to the severity of the CHOOZ constraint [12], it is possible that these results are not significantly altered in the presence of a fourth (sterile) neutrino flavour.

It may be pointed out that other analyses [2] find all three allowed regions, LMA, SMA and LOW. While the Ga experiments yield one data point (since it is an energy integrated measurement), the SNO and Super-Kamiokande experiments correspond to many points because of energy information. It is possible that the significance of the Ga data is reduced when doing a combined χ^2 analysis of such a data set.

A combination of the Ga, Cl and SNO (integrated) data can be used to determine certain "energy-averaged" values of P_{ee} [7]. For example, a constant P_{ee} corresponding to the SNO data at an average energy $\langle E_\nu \rangle = 10.8$ MeV may be assumed. Then the SNO data determine the value of P_{ee} at this energy. Assuming that this value holds for all ^8B neutrinos, we obtain the central value, $P_{ee}(E_\nu^{\text{B}}) = 0.347$ from SNO data. The Cl data has contributions from the ^8B flux as well as the ^7Be flux. Using $P_{ee}(E_\nu^{\text{B}})$, we obtain $P_{ee}(E_\nu^{\text{Be}}) = 0.29$; finally, using these values in the Ga data, the average survival probability in the pp region is obtained to be $P_{ee}(E_\nu^{\text{pp}}) = 0.76$. Since $\langle E_\nu^{\text{pp}} \rangle = 0.3$ MeV, and $E_\nu^{\text{Be}} = 0.86$ MeV, while $\langle E_\nu^{\text{B}} \rangle \sim 9$ MeV, it therefore appears as though there is a large energy dependence of P_{ee} in the lower energy $E_\nu < 1$ MeV regime. However, it is crucial to realise that this simplistic analysis may not hold when a detailed energy analysis is considered. For example the LMA solution that we have obtained corresponds to a flatter P_{ee} around 0.6 in this low energy region while

the SMA corresponds to a steeper one with an almost vanishing $P_{ee}(E_\nu^{\text{Be}})$. In either case the energy averaged predictions do not hold in detail. A completely unambiguous determination of P_{ee} in the $E_\nu < 1$ MeV regime must therefore await either results from Borexino or some new energy-sensitive data in the pp sector.

ACKNOWLEDGMENTS

We thank K. Kubodera, S. Nakamura and T. Sato for information on the deuterium cross-sections, Jimmy Law for discussions on the SNO data, and G. Rajasekaran for a critical reading of the manuscript.

REFERENCES

- [1] SNO Collab., Q.R. Ahmad et al., Phys. Rev. Lett. **87**, 071301 (2001); nucl-ex/0106015. The data tables are from the web-site, <http://ewiserver.npl.washington.edu/sno/>.
- [2] For example, see G.L. Fogli, E. Lisi, D. Montanino, and A. Palazzo, Phys. Rev. **D 64**, 093007 (2001); J.N. Bahcall, M.C. Gonzalez-Garcia, C. Pena-Garay, JHEP **0108**, 014 (2001); A. Bandyopadhyay, S. Choubey, S. Goswami, and K. Kar, Phys. Lett. **B 519**, 83 (2001); P.I. Krastev, A.Yu. Smirnov, preprint hep-ph/0108177.
- [3] SAGE Collab., J.N. Abdurashitov et al., Phys. Rev. Lett. **83**, 4686 (1999).
- [4] GNO Collab., M. Altmann et al., Phys. Lett. **B 490**, 16 (2000).
- [5] B.T. Cleveland et al., Astrophys. J. **496**, 505 (1998).
- [6] J.N. Bahcall, M.H. Pinsonneault and S. Basu, Astrophys J. **555**, 990 (2001). The data tables are taken from the web-site <http://www.sns.ias.edu/~jnb/index.html>.
- [7] V. Barger, D. Marfatia, and K. Whisnant, preprint hep-ph/0106207; V. Berezinsky, M. Lissia, Phys. Lett. **B 521**, 287 (2001).
- [8] T.K. Kuo and J. Pantaleone, Phys. Rev. **D 35**, 3432 (1987).
- [9] J.N. Bahcall, Phys. Rev. **C 56**, 3391 (1997); hep-ph/9710491.
- [10] S. Nakamura, T. Sato, V. Gudkov, and K. Kubodera, Phys. Rev. **C 63**, 034617 (2001). The data tables are available at <http://nuc003.psc.sc.edu/~kubodera/NU-D-NSGK>.
- [11] M. Apollonio et al., CHOOZ Collab., Phys. Lett. **B 420**, 397 (1998); Phys. Lett. **B 466**, 415 (1999) (hep-ex/9907037).
- [12] Gautam Dutta, D. Indumathi, M.V.N. Murthy, and G. Rajasekaran, Phys. Rev. **D 64**, 073011 (2001).

FIGURES

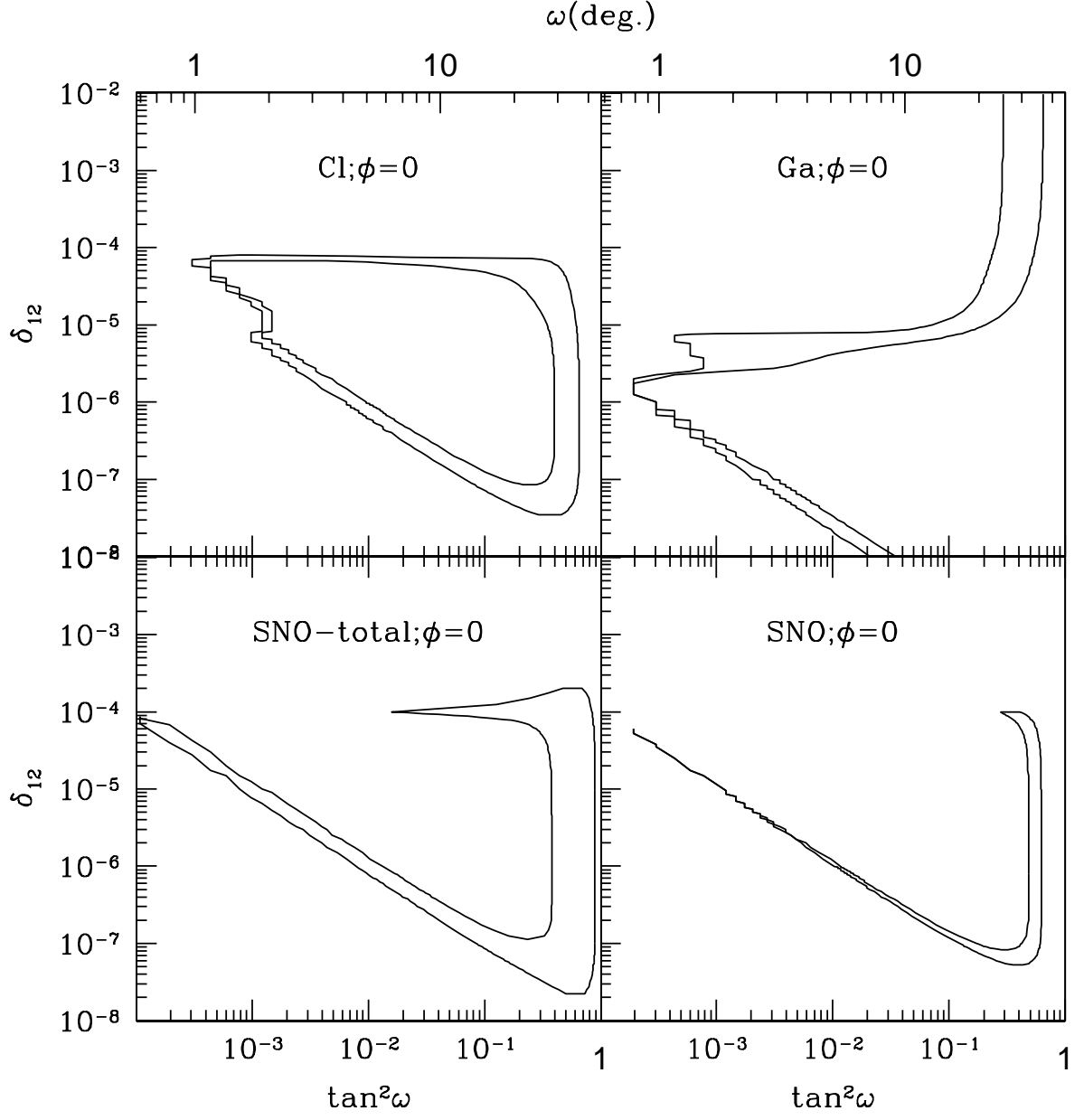


FIG. 1. 1σ allowed contours at $\phi = 0$ for the individual Chlorine, Gallium and SNO data sets. Results for the SNO total integrated data as well as for the energy-binned data are separately shown in the bottom panels.

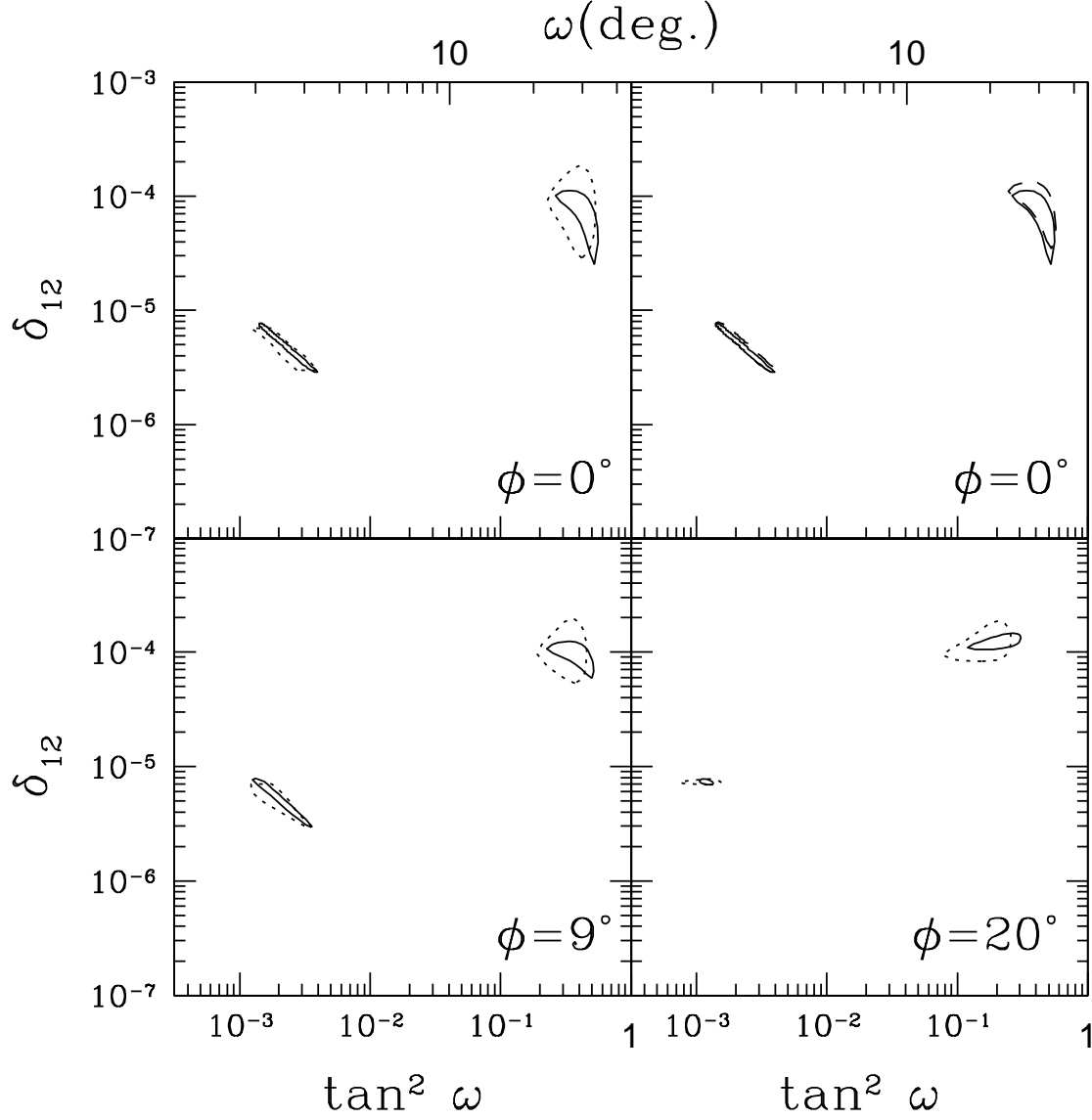


FIG. 2. Allowed 1σ regions in δ_{12} and the (12) mixing angle ω (both ω and $\tan^2 \omega$ are shown) parameter space for the combined Gallium and SNO data sets. The solid lines use the energy-binned SNO data while the dotted lines use the integrated SNO data. Allowed regions are shown for fixed values of $\phi = 0, 9, 20$ degrees. It is seen that the allowed region shrinks with increasing ϕ . The top right panel shows the fits (at $\phi = 0^\circ$) obtained by using all the SNO binned data (solid lines) and that from excluding the first four bins where correlated errors are large (dashed lines).

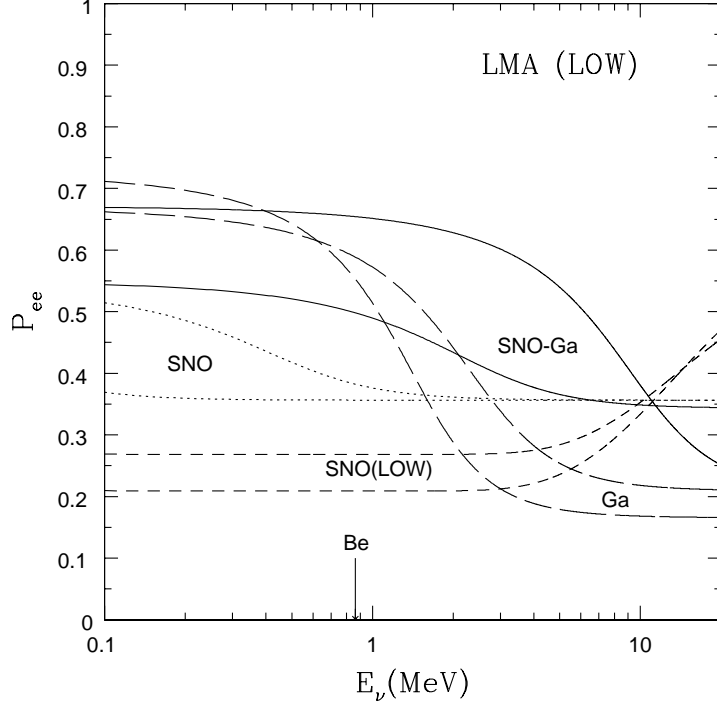


FIG. 3. The electron neutrino survival probability P_{ee} as a function of neutrino energy for the best fit solution in the LMA/LOW regions for $\phi = 0^\circ$. Two sets of lines for each solution indicate the 1σ band in the parameters. Solutions to individual SNO and Ga data are shown as dotted and long-dashed lines; the SNO LOW solution is shown as dashed lines. The solid lines indicate the preferred P_{ee} from fits to the combined Gallium and SNO data sets.

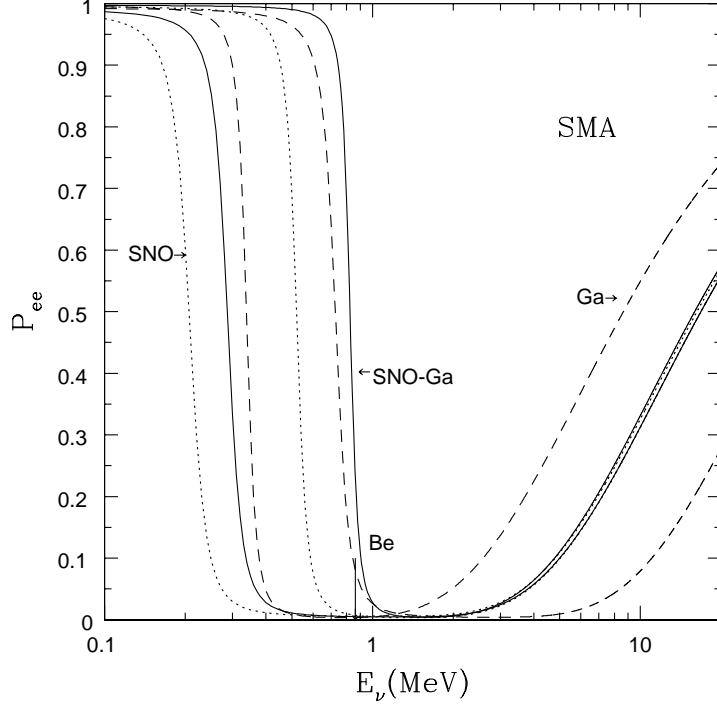


FIG. 4. The electron neutrino survival probability P_{ee} as a function of neutrino energy for the best fit solution in the SMA region for $\phi = 0^\circ$. Two sets of lines for each solution indicate the 1σ band in the parameters. Solutions to individual SNO and Ga data are shown as dotted and long-dashed lines. The solid lines indicate the preferred P_{ee} from fits to the combined Gallium and SNO data sets.

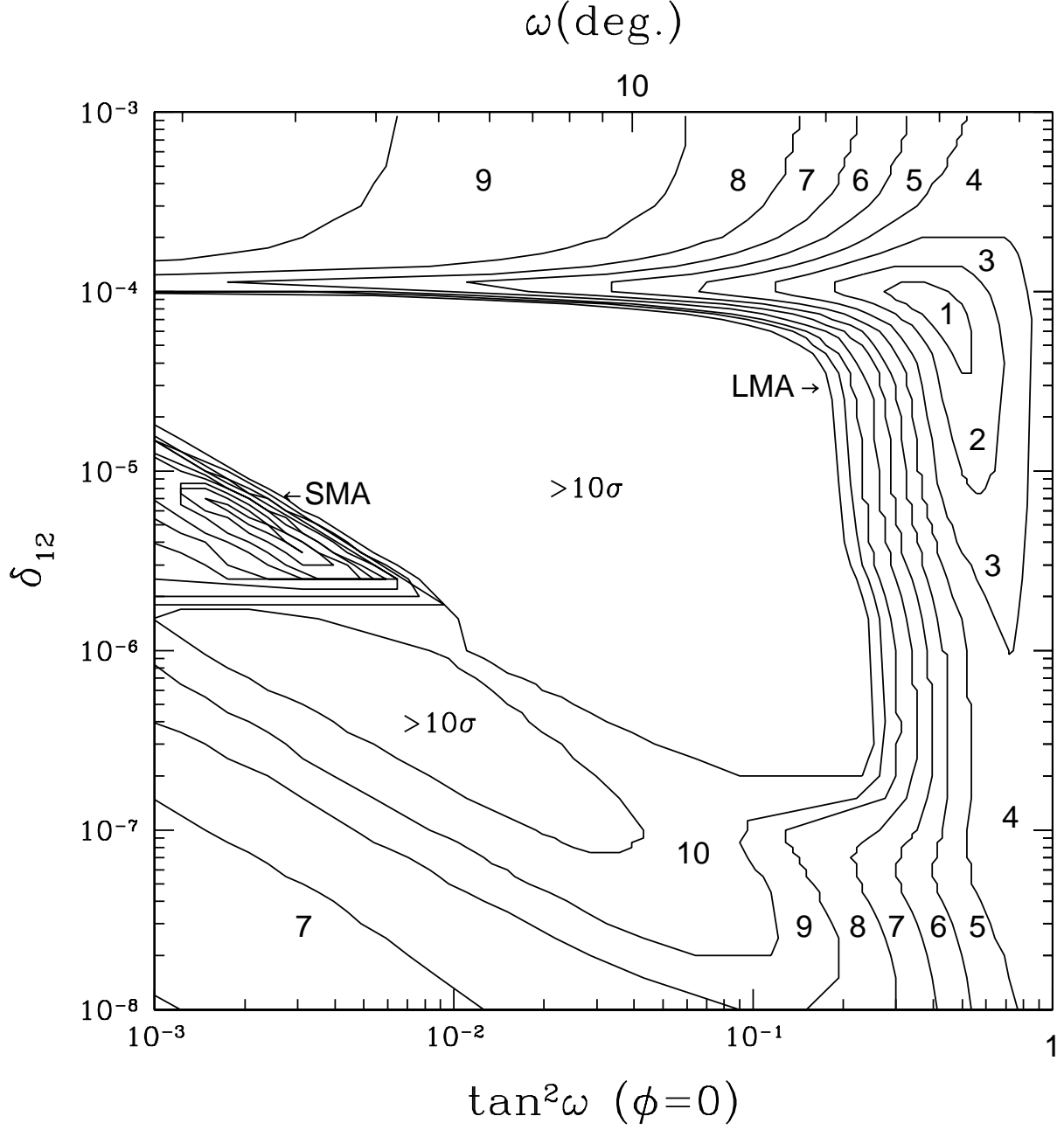


FIG. 5. Likelihood contours in the δ_{12} - $\tan^2 \omega$ plane for $\phi = 0^\circ$ corresponding to $n\sigma$ deviations, $n = 1, 10$, from the global minimum value of χ^2 for the combined Ga and SNO data fits. The LMA and SMA allowed regions are marked. The central regions of the parameter space are excluded by more than 10σ .

TABLES

δ_{12}	ω	ϕ	χ^2
$(8.5(-5.9, +2.8)) \times 10^{-5}$	$32.0(-4.9, +4.7)$	0	3.1
$(5.9(-3.1, +2.1)) \times 10^{-6}$	$2.5(-0.4, +1.2)$	0	2.6
$(1.0(-0.4, +0.2)) \times 10^{-4}$	$30.2(-4.8, +5.6)$	9	3.3
$(7.2(-1.6, +0.7)) \times 10^{-6}$	$2.2(-0.2, +1.3)$	9	2.6
$(1.2(-0.1, +0.3)) \times 10^{-4}$	$23.9(-4.8, +5.0)$	20	3.9
$(7.3(-0.4, +0.5)) \times 10^{-6}$	$2.0(-0.1, +0.1)$	20	2.4
$(8.7(-6.1, +4.8)) \times 10^{-5}$	$32.1(-10.9, +4.9)$	$0.003(-23.0, +23.0)$	2.8

TABLE I. Values of δ_{12} and ω corresponding to χ^2 minima for the combined fits to SNO and Ga data for different fixed values of ϕ . 1σ errors on the parameter values are also given. The last row corresponds to a global minimum with respect to all three parameters, δ_{12} , ω , and ϕ .